A Novel Fluorine-Containing Graft Copolymer Bearing Perfluorocyclobutyl Aryl Ether-Based Backbone and Poly(methyl methacrylate) Side Chains

HAO LIU,[1] YONGJUN LI,[1] SEN ZHANG,[1] DONG YANG,[2] JIANHUA HU,[2] XIAOYU HUANG[1]

[1]Key Laboratory of Organofluorine Chemistry and Laboratory of Polymer Materials, Shanghai Institute of Organic Chemistry, Chinese Academy of Sciences, 345 Lingling Road, Shanghai 200032, People's Republic of China

[2]Key Laboratory of Molecular Engineering of Polymers (Ministry of Education), Laboratory of Advanced Materials and Department of Macromolecular Science, Fudan University, 220 Handan Road, Shanghai 200433, People's Republic of China

Received 25 August 2010; accepted 27 August 2010
DOI: 10.1002/pola.24352
Published online 13 October 2010 in Wiley Online Library (wileyonlinelibrary.com).

ABSTRACT: A series of novel graft copolymers consisting of perfluorocyclobutyl aryl ether-based backbone and poly(methyl methacrylate) side chains were synthesized by the combination of thermal [$2\pi + 2\pi$] step-growth cycloaddition polymerization of aryl bistrifluorovinyl ether monomer and atom transfer radical polymerization (ATRP) of methyl methacrylate. A new aryl bistrifluorovinyl ether monomer, 2-methyl-1,4-bistrifluorovinyloxybenzene, was first synthesized in two steps from commercially available reagents, and this monomer was homopolymerized in diphenyl ether to provide the corresponding perfluorocyclobutyl aryl ether-based homopolymer with methoxyl end groups. The fluoropolymer was then converted to ATRP macroinitiator by the monobromination of the pendant methyls with *N*-bromosuccinimide and benzoyl peroxide. The grafting-from strategy was finally used to obtain the novel poly(2-methyl-1,4-bistrifluorovinyloxybenzene)-*g*-poly(methyl methacrylate) graft copolymers with relatively narrow molecular weight distributions ($M_w/M_n \leq 1.46$) via ATRP of methyl methacrylate at 50 °C in anisole initiated by the Br-containing macroinitiator using CuBr/dHbpy as catalytic system. These fluorine-containing graft copolymers can dissolve in most organic solvents. This is the first example of the graft copolymer possessing perfluorocyclobutyl aryl ether-based backbone. © 2010 Wiley Periodicals, Inc. J Polym Sci Part A: Polym Chem 49: 11–22, 2011

KEYWORDS: atom transfer radical polymerization (ATRP); fluoropolymers; graft copolymers; grafting-from; perfluorocyclobutyl aryl ether

INTRODUCTION High-performance fluoropolymers possessing many advantages[1] including the increased thermal and oxidative stability, optical transparency, solvent compatibility, and environmental stability have been extensively applied in many different fields since the first example of fluoropolymer, polytetrafluoroethylene (PTFE), was discovered by Plunkett of DuPont in 1938.[2] For example, Percec et al.[3–15] reported fluorinated liquid crystal molecules with perfluorinated alkane chains, which could result in a microsegregation at the molecular levels, and this process alone could be responsible for the formation of lamellar thermotropic and lyotropic mesophases. These unique properties compared with those of usual carbon–hydrogen–oxygen-containing polymers originate from the incorporation of fluorocarbon functionality. However, the solubility and processability of fluoropolymers are generally low due to the high crystallinity, which certainly limited their applications. Thus, many partially fluorinated polymers with low crystallinity, such as polychlorotrifluoroethylene, Teflon-AF, Cytop, and various copolymers of PTFE, have been developed to improve the processability.[1] In particular, perfluorocyclobutyl (PFCB) aryl ether polymers have received considerable attention since its discovery by Babb et al. of Dow Chemical Co. in early 1990s.[16,17] They are synthesized by the predominant head-to-head thermal [$2\pi + 2\pi$] step-growth cyclopolymerization of aryl trifluorovinyl ethers (TFVE) above 150 °C free of any initiator and catalyst, which first proceeds to form a stable diradical intermediate followed by rapid ring closure to provide a mixture of *cis*- and *trans*-1,2-disubstituted perfluorocyclobutanes.[18–20] This relatively new class of semifluorinated polymers exhibit not only high thermal/oxidative stability, chemical resistance, and superior electrical insulating ability but also improved processability compared with traditional fluoropolymers.[21–24] Thus, PFCB-containing polymers are attractive for a multitude of new applications due to the combination of solution processability and thermal stability as reviewed by Smith et al.[24]

Most recent studies of PFCB-based polymers focused on the thermal polymerization of different bis- and trifunctionalized aryl TFVE monomers to obtain diverse thermoplastic and thermoset homopolymers and random copolymers bearing PFCB aromatic ether linkages,[19,20,25–38] in which PFCB connection was used as a way to link different functionalities

Correspondence to: X. Huang (E-mail: xyhuang@mail.sioc.ac.cn) or D. Yang (E-mail: yangdong@fudan.edu.cn)

for meeting various demands of applications such as hole-transporting material,[25,26] optical waveguide applications,[28,29] curing additive,[18] proton exchange membrane,[35,36] light emission,[37] and light-optic[38] applications. However, the cases about the synthesis of PFCB aryl ether-based copolymers via aryl TFVE and commonly used vinyl monomers are very limited because of the peculiar radical-mediated polymerization mechanism ([$2\pi + 2\pi$] cycloaddition) and relatively high polymerization temperature (at least >150 °C).[39–42] Therefore, to widen the application scope of PFCB aryl ether-based fluoropolymer, it is necessary to combine the high performance of PFCB aryl ether-based fluoropolymer with other commercial polymer.

Graft copolymers with a stable covalent connection between the backbone and the side chains may be a suitable choice to implement the above consideration. In general, graft copolymers are synthesized via three different routes: grafting-through, grafting-onto, and grafting-from strategies.[43] The grafting-through strategy is to prepare graft copolymers via the polymerization of the macromonomers with a polymerizable end group; a broad chain length distribution existed in the graft copolymers yielded by the traditional free radical polymerization of the macromonomers[44] and the living polymerization of the macromonomers afforded well-defined graft copolymers with low molecular weights.[45] The grafting-onto technique is based on attaching certain side chains onto a linear backbone by a coupling reaction,[46–51] which requires a high coupling efficiency between the backbone and the side chains. The grafting-from approach utilizes the pendant initiation sites on the backbone, i.e., macroinitiator, which can be obtained directly from the initiation group-containing monomer or by the introduction of initiating functional groups to a precursor, to initiate the polymerization of another monomer to form the side chains.[52,53] With the advent of living/controlled polymerization technique, especially living/controlled radical polymerization including atom transfer radical polymerization (ATRP),[53–57] modified ATRP,[58] single-electron transfer living radical polymerization (SET-LRP),[59–63] and reversible addition fragmentation chain transfer (RAFT),[64,65] this method is considered as a particularly attractive procedure to synthesize well-defined graft copolymers because low instantaneous propagating species limit the coupling and termination reactions and the gradual growth of side chains can effectively decrease the steric effect that is inevitable for "grafting-onto" and "grafting-through" strategies. Many graft copolymers with various backbones and side chains have been prepared by combining the grafting-from strategy with living polymerization.[52,53,66–73] Specifically, the side chains can be formed in a well-defined way via ATRP through the grafting-from approach and the living nature of ATRP enabled it to control both the molecular weights and molecular weight distributions of the side chains.[52,64–68,71,73]

Until now, none has reported the graft copolymer consisting of PFCB aryl ether segment. In this work, we present the first example of PFCB aryl ether-based graft polymer with poly(methyl methacrylate) (PMMA) side chains. PFCB aryl ether-based backbone was prepared by the thermal step-growth cyclopolymerization of a new aryl bistrifluorovinyl ether monomer, 2-methyl-1,4-bistrifluorovinyloxybenzene (MBTVFB). ATRP initiation groups were introduced into the backbone by the monobromination of the pendant methyls. The target graft copolymer, poly(2-methyl-1,4-bistrifluorovinyloxybenzene)-*g*-poly(methyl methacrylate) (PMBTFVB-*g*-PMMA), was synthesized via ATRP graft copolymerization of methyl methacrylate.

EXPERIMENTAL

Materials

Methyl methacrylate (MMA, Aldrich, 99%) was washed with 5% aqueous NaOH solution to remove the inhibitor and then with water, dried over $MgSO_4$, and distilled twice from CaH_2 under reduced pressure prior to use. CuBr (Aldrich, 98%) was purified by stirring overnight over CH_3CO_2H at room temperature, followed by washing the solid with ethanol, diethyl ether, and acetone prior to drying *in vacuo* at 40 °C for 1 day. Granular zinc (Aldrich, 99.99%) was activated by washing in 0.1 M HCl followed by drying *in vacuo* at 140 °C for 10 h. Toluene (Aldrich, 99%) was dried over CaH_2 and distilled from sodium and benzophenone under N_2 prior to use. Anisole (Aldrich, 99%) and diphenyl ether (Aldrich, 99%) were dried over CaH_2 and distilled under reduced pressure prior to use. *N*-Bromosuccinimide (NBS, Aldrich, 99%) was recrystallized from water and dried *in vacuo* at 35 °C for 1 day. Benzoyl peroxide (BPO, Alfa Aesar, 97%) was purified by dissolving in acetone and precipitating in water followed by drying *in vacuo* at room temperature for 1 day. $BrCF_2CF_2Br$ was prepared by condensing equimolar amounts of bromine and tetrafluoroethylene at −195 °C followed by warming up to 22 °C.[74] 4-Methoxytrifluorovinyloxybenzene[23] and diheptyl-2,2′-bipyridine (dHbpy)[75] were prepared according to previous literatures. 2-Methylhydroquinone (Aldrich, 99%), CH_3CN (Aldrich, 99.8%), CCl_4 (Aldrich, 99.5%), dimethyl sulfoxide (DMSO, Aldrich, 99.9%), and KOH (Aldrich, 90%) were used as received.

Measurements

FT-IR spectra were recorded on a Nicolet AVATAR-360 FT-IR spectrophotometer with a resolution of 4 cm^{-1}. All NMR analyses were performed on a Bruker AM-300 spectrometer (300 MHz) in $CDCl_3$, TMS (^1H NMR) and $CDCl_3$ (^{13}C NMR) were used as internal standards, and CF_3CO_2H was used as external standard for ^{19}F NMR. EI-MS and HRMS were measured by an Agilent 5937N system and a Waters Micromass GCT instrument, respectively. The bromine content was determined by the titration with $Hg(NO_3)_2$. Relative molecular weights and molecular weight distributions were measured by conventional gel permeation chromatography (GPC) system equipped with a Waters 1515 Isocratic HPLC pump, a Waters 2414 refractive index detector, and a set of Waters Styragel columns [HR3 (500-30,000), HR4 (5000-600,000) and HR5 (50,000-4,000,000) 7.8 × 300 mm, particle size: 5 μm]. GPC measurements were carried out at 35 °C using tetrahydrofuran (THF) as eluent with a flow rate of 1.0 mL/min. The system was calibrated with linear polystyrene

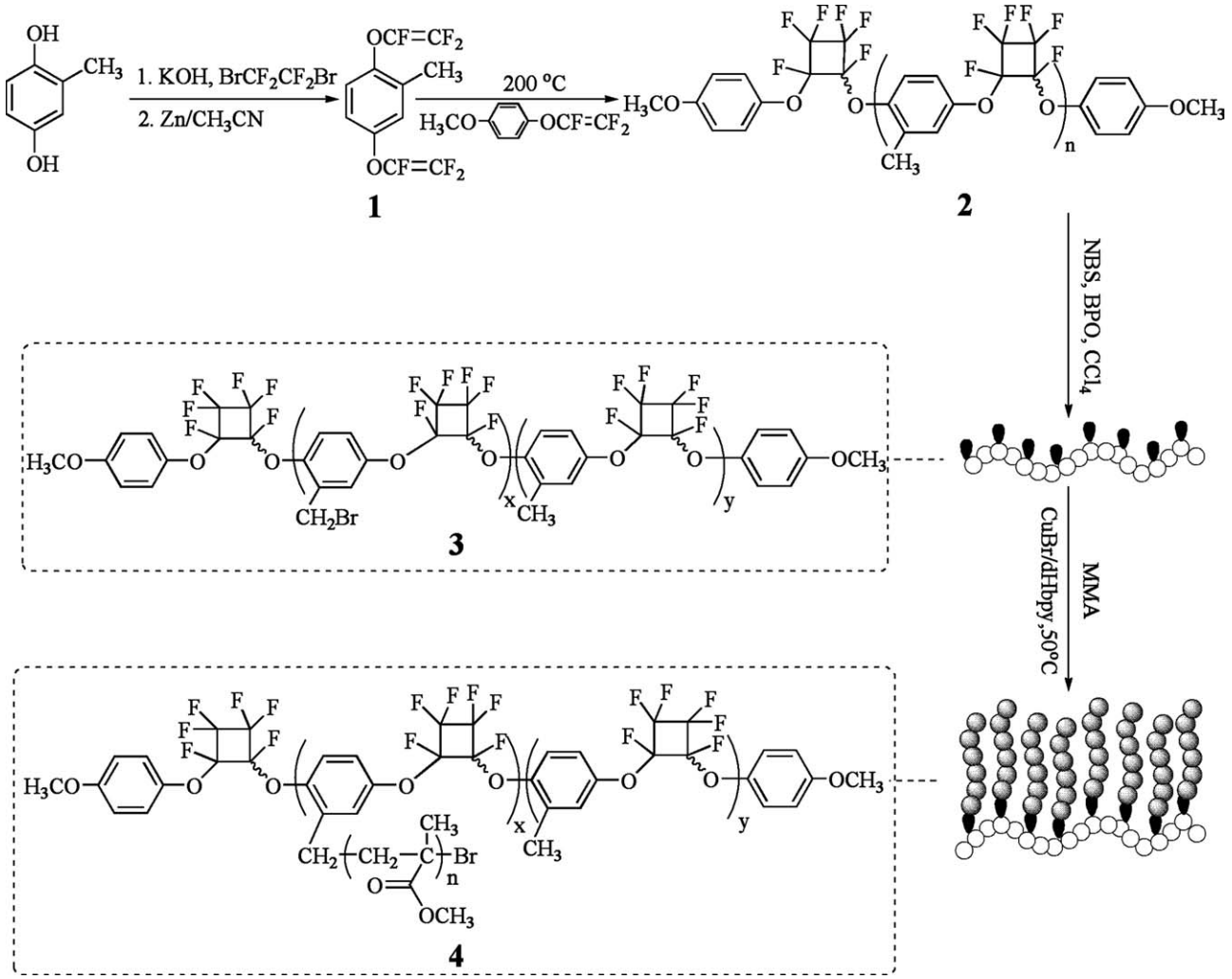

SCHEME 1 Synthesis of PMBTFVB-*g*-PMMA graft copolymer.

standards. Conversions of MMA were determined by GC using a HP 6890 system with an SE-54 column, and anisole was used as internal standard. Differential scanning calorimetry (DSC) measurements were run on a TA Q200 system under N_2 purge with a heating rate of 10 °C/min. The glass transition temperature (T_g) was recorded from the second heating process after a quick cooling from 200 °C, and the value was determined from the midpoint of C_p curve. Thermogravimetric analysis (TGA) measurements were run on a TA Q500 system under N_2 purge with a heating rate of 10 °C/min. The decomposition temperature (T_d) is defined as the temperature with 10% weight loss.

Synthesis of Aryl Bistrifluorovinyl Ether Monomer

MBTVFB **1** was synthesized in two steps using 2-methylhydroquinone as starting material (Scheme 1). 2-Methylhydroquinone (12.41 g, 0.10 mol), toluene (120 mL), and DMSO (150 mL) were first introduced to a 500 mL three-neck flask (flame-dried prior to use) fitted with a N_2 inlet and a Barrett trap topped with a reflux condenser. The solution was deoxygenated by introducing N_2 for 30 min followed by adding KOH (12.44 g, 90%, 0.20 mol). The mixture was refluxed at 180 °C to azeotropically remove the water until no more water was collected in the trap. The solution was then cooled to below 15 °C and $BrCF_2CF_2Br$ (30 mL, 0.25 mol) was added dropwise in 1 h. The mixture was warmed to room temperature for 12 h and heated to 35 °C for another 8 h. The reaction was quenched with water and the mixture was extracted with CH_2Cl_2. All organic layers were collected and dried over $MgSO_4$. The intermediate, 19.76 g (40.9%) of 2-methyl-1,4-bis(2-bromotetrafluoroethoxy)phenyl (clear oil), was obtained by silica column chromatography. ^{1}H NMR (300 MHz): δ (ppm): 2.24 (3H, CH_3), 7.08, 7.13, 7.24 (3H, phenyl). HR-MS: $C_{11}H_6O_2Br_2F_8$: calcd 479.8607, found 479.8604.

Zinc (11.44 g, 0.176 mmol) was first introduced to a 250 mL three-neck flask (flame-dried prior to use) fitted with a reflux condenser. After three cycles of evacuating and backfilling with N_2, CH_3CN (120 mL) was charged via a gastight syringe and the mixture was refluxed at 110 °C. The above-prepared intermediate, 2-methyl-1,4-bis(2-bromotetrafluoroethoxy)phenyl (24.19 g, 0.05 mmol), was added dropwise

in 1 h and the mixture was refluxed at 110 °C for 10 h. After cooling to room temperature, the suspending zinc salt was removed by the filtration. The filtrate was washed by water and dried over $MgSO_4$. The crude product was purified by silica column chromatography to obtain 9.20 g (65.0%) of MBTFVB **1** (clear oil). FT-IR: ν (cm^{-1}): 3045, 2968, 1833, 1600, 1496, 1422, 1315, 1279, 1179, 1157, 1009, 945, 874, 808, 767. ^{1}H NMR (300 MHz): δ (ppm): 2.33 (s, 3H, CH_3), 6.93 (d, J = 8.8 Hz, 1H, phenyl), 6.97 (s, 1H, phenyl), 7.01 (d, J = 8.8 Hz, 1H, phenyl). ^{13}C NMR (75 MHz): δ (ppm): 15.7 (*C*H_3), 114.3, 115.5, 119.0, 129.9 (phenyl), 132.8, 135.2, 143.9, 144.4, 146.5, 147,1, 149.3, 149.9 (O*C*F=*C*F_2), 150.3, 151.6 (phenyl). ^{19}F NMR (282 MHz): δ (ppm): −120.3, −127.0, −134.3. EI-MS: m/z (%): 284 ([M]$^+$, 100.00), 187 (20.49), 159 (11.81), 140 (24.04), 119 (17.50), 109 (32.77), 90 (83.16), 77 (4.09), 51 (7.58). HR-MS: $C_{11}H_6O_2F_6$: calcd 284.0272, found, 284.0268.

Thermal Homopolymerization of MBTFVB

PMBTFVB **2** homopolymer was synthesized via the thermal step-growth cycloaddition polymerization of aryl bistrifluorovinyl ether monomer **1**. MBTFVB **1** (8.00 g, 28.16 mmol) and diphenyl ether (16 mL) were added to a 50 mL Schlenk flask (flame-dried under vacuum prior to use) sealed with a rubber septum under N_2. The flask was degassed by three cycles of freezing–pumping–thawing followed by immersing the flask into an oil bath thermostated at 200 °C. 4-Methoxytrifluoro-vinyloxybenzene (2.87 g, 14.07 mmol) was charged via a gastight syringe after 4 h. The polymerization was terminated by putting the flask into liquid N_2 after another 6 h. THF (15 mL) was added to the flask for dilution, and the resulting solution was precipitated into methanol. After repeated purification by dissolving in THF and precipitating in methanol, 4.53 g (56.6%) of white powder, PMBTFVB **2** homopolymer, was obtained after drying *in vacuo* overnight. GPC: M_n = 4600 g/mol, M_w/M_n = 1.27, FT-IR: ν (cm^{-1}): 3053, 2933, 1599, 1498, 1315, 1267, 1203, 1120, 1009, 962, 925, 813, 743. ^{1}H NMR (300 MHz): δ (ppm): 2.06, 2.27 (3H, CH_3), 3.77 (3H, OCH_3), 6.97, 7.10 (3H, phenyl). ^{13}C NMR (75 MHz): δ (ppm): 16.0 (*C*H_3), 55.4 (O*C*H_3), 105.7, 109.2, 112.7 (4C, PFCB), 116.5, 121.5, 131.0, 148.3 (phenyl). ^{19}F NMR (282 MHz): δ (ppm): −128.3 to −132.2 (6F, PFCB).

Monobromination of PMBTFVB

The pendant methyls of PMBTFVB **2** homopolymer were monobrominated by NBS and BPO. In a typical procedure, PMBTFVB **2** (M_n = 4600 g/mol, M_w/M_n = 1.27, 2.00 g, 7.04 mmol CH_3 group), NBS (0.8771 g, 4.93 mmol), BPO (0.3110 g, 1.28 mmol) were first added to a 1000 mL three-neck flask (flame-dried prior to use) fitted with a reflux condenser followed by deoxygenating under N_2. CCl_4 (400 mL) was charged via a gastight syringe and the solution was refluxed at 80 °C for 1 day. After filtration, CCl_4 was removed from the filtrate using a rotary evaporator. The obtained solid was dissolved in ethyl acetate (500 mL), and the resulting solution was washed with distilled water (200 mL ×2) followed by drying over $MgSO_4$. The solution was concentrated and precipitated into methanol. After repeated purification by dissolving in THF and precipitating in methanol, 0.9467 g of white powder, PMBTFVB-Br **3a** macroinitiator, was obtained after drying *in vacuo* overnight. GPC: M_n = 5700 g/mol, M_w/M_n = 1.18. EA: Br%: 12.34%. ^{1}H NMR (300 MHz): δ (ppm): 1.99, 2.18 (3H, CH_3), 3.68 (3H, OCH_3), 4.17, 4.34 (2H, CH_2Br), 6.86, 7.04, 7.16 (3H, phenyl). ^{13}C NMR (75 MHz): δ (ppm): 15.3 (*C*H_3), 24.6 (*C*H_2Br), 54.7 (OCH_3), 105.0, 107.8, 111.7 (4C, PFCB), 116.5, 118.7, 120.8, 129.3, 148.1 (phenyl). ^{19}F NMR (282 MHz): δ (ppm): −127.1 to −132.7 (6F, PFCB).

ATRP Graft Copolymerization of MMA

ATRP graft copolymerization of MMA was initiated by PMBTFVB-Br **3** macroinitiator using CuBr/dHbpy as catalytic system. In a typical procedure, PMBTFVB-Br **3a** (M_n = 5700 g/mol, M_w/M_n = 1.18, Br% = 12.34%, 31.7 mg, 0.0489 mmol Br group), CuBr (7.0 mg, 0.0488 mmol), and dHbpy (34.4 mg, 0.0976 mmol) were first added to a 25 mL Schlenk flask (flame-dried under vacuum prior to use) sealed with a rubber septum for degassing and kept under N_2. Next, MMA (1.30 mL, 12.2 mmol) and anisole (1.30 mL) were introduced via a gastight syringe. The flask was degassed by three cycles of freezing–pumping–thawing, and the mixture was stirred at room temperature for 10 min so that the mixture became homogeneous. The flask was immersed into an oil bath preset at 50 °C to start the polymerization. The polymerization was terminated by putting the flask into liquid N_2 after 3.5 h. The reaction mixture was diluted by THF and passed through an Al_2O_3 column to remove the residual copper catalyst. The solution was concentrated and precipitated into methanol. After repeated purification by dissolving in THF and precipitating in methanol, 0.2854 g of white powder, PMBTFVB-*g*-PMMA **4d** graft copolymer, was obtained after drying *in vacuo* overnight. GPC: M_n = 79,500 g/mol, M_w/M_n = 1.29. FT-IR: ν (cm^{-1}): 2994, 2951, 2926, 2856, 1730, 1483, 1449, 1388, 1271, 1240, 1191, 1148, 1066, 964, 842, 749. ^{1}H NMR (300 MHz): δ (ppm): 0.84, 1.02, 1.25 (3H, CCH_3), 1.45, 1.60, 1.81 (2H, CH_2 of PMMA side chain), 1.89 (2H, CH_2 connected to the aryl), 2.07, 2.27 (3H, CH_3), 3.60 (3H, COOCH_3), 3.82 (3H, OCH_3), 6.91, 7.02, 7.11 (3H, phenyl). ^{19}F NMR (282 MHz): δ (ppm): −128.1 to −132.2 (6F, PFCB).

RESULTS AND DISCUSSION

Synthesis of MBTFVB Monomer

MBTVFB **1** aryl bistrifluorovinyl ether monomer was synthesized from commercially available 2-methylhydroquinone in two steps with a total yield of 26.6% via the fluoroalkylation with $BrCF_2CF_2Br$ followed by Zn-mediated elimination according to the conventional approach.[76–78] FT-IR, ^{1}H NMR, ^{19}F NMR, and ^{13}C NMR were used to characterize the chemical structure of this monomer. The characteristic signal of the trifluorovinyl located at 1833 cm^{-1} in FT-IR spectrum of MBTFVB **1** [Fig. 1(A)]. The peaks at 1600, 1496, 808, and 1179 cm^{-1} were attributed to the benzene ring and the ether bond, respectively. Figure 2(A) shows ^{1}H NMR spectrum of MBTFVB **1** and the typical resonance signal of the methyl located at 2.33 ppm. A series of peaks around 7.00 ppm corresponded to three protons of the benzene ring. The singlet at 6.97 ppm belonged to one proton

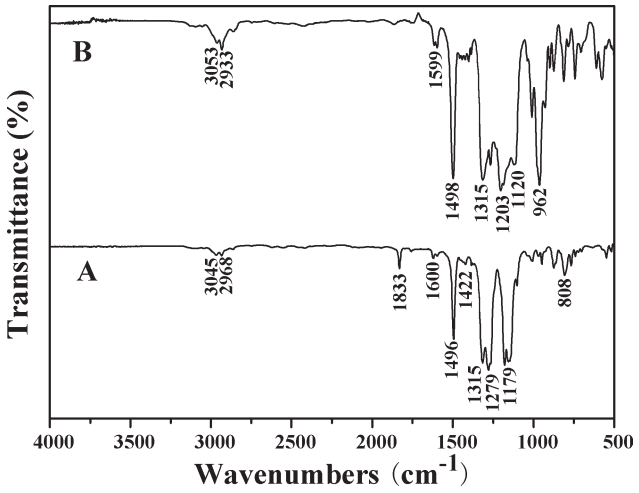

FIGURE 1 FT-IR spectra of MBTVFB **1** (A) and PMBTFVB **2** (B).

adjacent to the methyl. The signals of other two protons of benzene ring appeared at 6.93 and 7.01 ppm as two doublets, respectively. Moreover, the presence of the trifluorovinyl was demonstrated by three typical muitiplets at −120.3, −127.0, and −134.3 ppm[31,76] in ^{19}F NMR spectrum of MBTFVB **1** as shown in Figure 2(B). ^{13}C NMR spectrum of MBTVFB **1** is shown in Figure 2(C) and the peaks between 132.8 and 149.9 ppm were attributed to two carbons of the trifluorovinyl.[31,76] The signal at 15.7 ppm corresponded to the methyl and the peaks at 114.3, 115.5, 119.0, 129.9, 150.3, and 151.6 ppm originated from six carbons of the benzene ring.[31,76] HR-MS result (284.0268) also well accorded with the calculated value (284.0272). Thus, all the above results confirmed the successful synthesis of bistrifluorovinyl-containing monomer **1**.

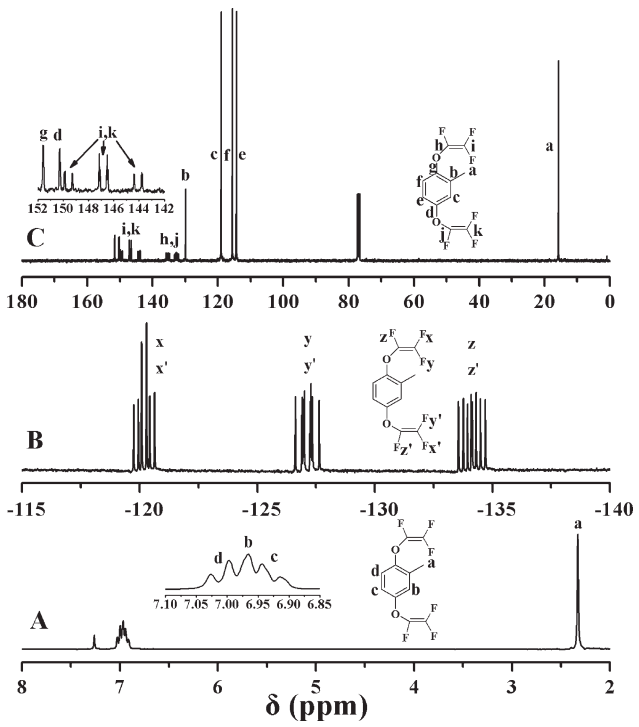

FIGURE 2 ^{1}H (A), ^{13}C (B), and ^{19}F NMR (C) spectra of MBTFVB **1** in $CDCl_3$.

Preparation of PFCB Aryl Ether-Based Backbone

Thermal [2π + 2π] step-growth cyclopolymerization of bifunctional MBTFVB **1** monomer was performed in diphenyl ether at 200 °C to afford PMBTFVB **2** homopolymer. Monofunctional 4-methoxytrifluorovinyloxybenzene was used as end-capping agent. This homopolymer was characterized by FT-IR, ^{1}H NMR, ^{13}C NMR, and ^{19}F NMR. After thermal homopolymerization, the typical peak of the trifluorovinyl at 1833 cm^{-1} in FT-IR spectrum completely disappeared [Fig. 1(B)] and a new sharp band of PFCB linkage appeared at 962 cm^{-1} in comparison with that of the monomer [Fig. 1(A)], which indicated the presence of PFCB linkage in homopolymer. ^{19}F NMR spectrum after thermal homopolymerization showed the disappearance of the representative signals of the trifluorovinyl, and new multiplets ranging from −128.3 to −132.2 ppm appeared instead, this also illustrating the existence of PFCB functionality. The singlets at 2.06 and 2.27 ppm in ^{1}H NMR spectrum after thermal homopolymerization [Fig. 3(A)] were attributed to three protons of the methyl and the broad peaks at 6.97 and 7.10 ppm corresponded to three protons of the benzene ring. Furthermore, the signal of three protons of terminal methoxyl was found to be located at 3.77 ppm as a singlet, which verified the effective end-capping with 4-methoxytrifluorovinyloxybenzene. Figure 4(A) shows ^{13}C NMR spectrum after thermal homopolymerization, and the signals of the trifluorovinyl disappeared compared with that of the monomer [Fig. 2(C)]. Instead, new peaks between 106.5 and 112.7 ppm attributed to four carbons of PFCB linkage appeared. Another new peak at 55.4 ppm belonged to the carbon of terminal methoxyl.

GPC measurement offered the relative molecular weight of PMBTFVB **2** (M_n = 4600 g/mol). Because GPC was

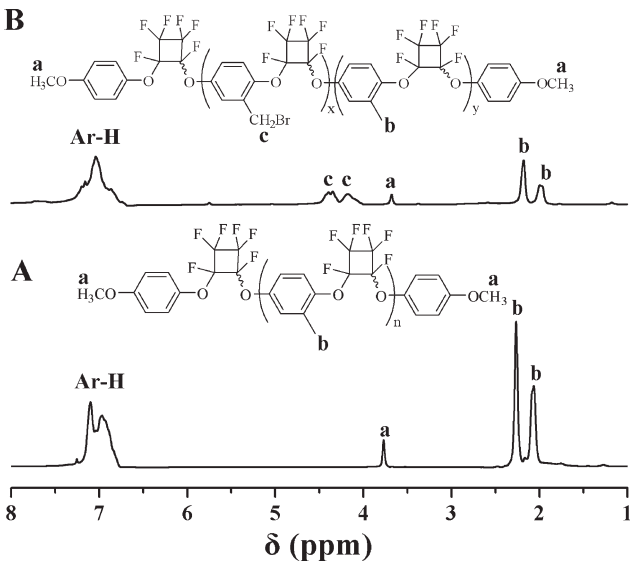

FIGURE 3 ^{1}H NMR spectra of PMBTFVB **2** (A) and PMBTFVB-Br **3** (B) in $CDCl_3$.

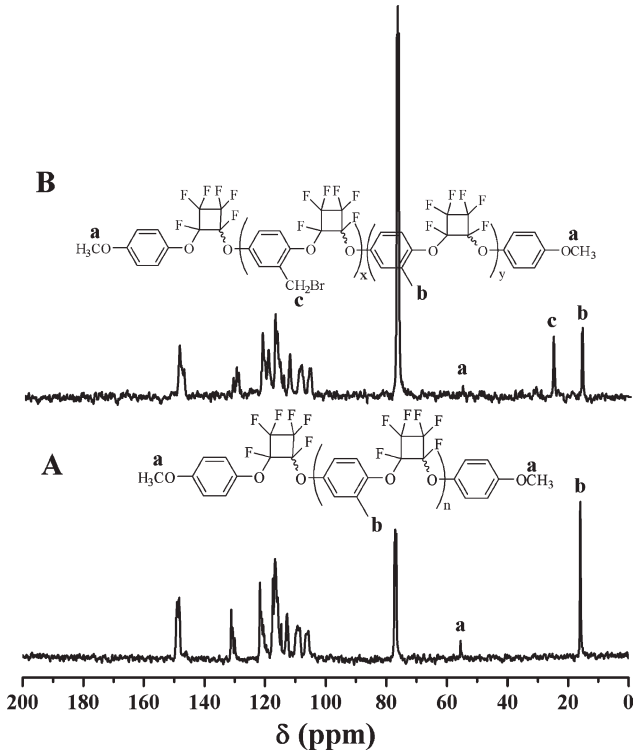

FIGURE 4 ^{13}C NMR spectra of PMBTFVB **2** (A) and PMBTFVB-Br **3** (B) in $CDCl_3$.

calibrated with linear polystyrene standards, ^1H NMR was used to determine the "absolute" molecular weight of the homopolymer. The molecular weight of PMBTFVB **2** ($M_{n,NMR}$) can be estimated according to eq 1 (S_a and S_b are the area of peak "a" at 3.77 ppm and peaks "b" at 2.06 and 2.27 ppm in Figure 3(A), respectively; 284 and 204 are the molecular weights of MBTFVB **1** and 4-methoxytrifluorovinyloxybenzene, respectively). The value of S_b/S_a is 15.5 and the molecular weight is calculated to be 9200 g/mol. This result shows that every PMBTFVB **2** chain possesses 31.0 repeating units.

$$M_{n,NMR} = 284 \times (2S_b/S_a) + 204 \times 2 \quad (1)$$

All these evidences confirmed the structure of PMBTFVB **2** homopolymer. In addition, this homopolymer is soluble in most common organic solvents such as THF, CH_2Cl_2, chloroform, hexane, cyclohexane, toluene, acetone, ethyl acetate, and DMF; however, it is insoluble in water and methanol.

Preparation of PMBTFVB-Br ATRP Macroinitiator

The pendant methyls of PMBTFVB **2** homopolymer were monobrominated by NBS and BPO using CCl_4 as solvent so that PMBTFVB **2** homopolymer was transformed into PMBTFVB-Br **3** macroinitiator. Two different feeding ratios of NBS to the methyls were used to tune the degree of bromination, and the bromine content increased with the raising of the adding amount of NBS as listed in Table 1. The changes of the bromine content for both samples (0%–12.34% for **3a** and 16.28% for **3b**, respectively) showed the presence of halogen-containing ATRP initiation group in both samples.[79] Both samples' molecular weights after the reaction with NBS and BPO were higher than that of the homopolymer, this also witnessing the occurrence of the bromination reaction.

The successful bromination was also confirmed by ^1H NMR and ^{13}C NMR. ^1H NMR spectrum after the reaction is shown in Figure 3(B) and two new peaks attributed to two protons of newly formed CH_2Br group appeared at 4.17 and 4.34 ppm. Moreover, a new peak originating from the carbon of CH_2Br group was found to be located at 24.6 ppm in ^{13}C NMR spectrum after the reaction as shown in Figure 4(B). The original signals of PMBTFVB **2** homopolymer were kept in ^1H NMR [Fig. 3(B)], ^{13}C NMR [Fig. 4(B)], and ^{19}F NMR spectra after the reaction, demonstrating that the polymeric architecture was not affected during the bromination. As we can see from Figure 5, unimodal and symmetrical GPC curves were found for both PMBTFVB-Br **3a** and **3b** macroinitiators, which also verified that the architecture of polymer chain was not altered during the bromination.[80]

From the data of Br% as listed in Table 1, the number of CH_2Br ATRP initiation group (N_{ATRP}) can be calculated according to the following equation set, in which "*x*" and "*y*" are the numbers of repeating unit with CH_2Br and CH_3 group as shown in Scheme 1, respectively; 80 is the molecular weight of bromine atom; 363 and 284 are the molecular weights of repeating unit with CH_2Br and CH_3 group, respectively; 204 is the molecular weight of 4-methoxytrifluorovinyloxybenzene; 31.0 is the number of repeating unit of PMBTFVB **2** homopolymer. The values of N_{ATRP} are 16.2 and 22.3 for PMBTFVB-Br **3a** and **3b**, respectively. The grafting densities of CH_2Br ATRP initiation group (D_{ATRP}) are

TABLE 1 Preparation of PMBTFVB-Br **3** Macroinitiator[a]

Sample	NBS (eq.)	Br%[b]	$M_{n,GPC}$[c] (KDa)	M_w/M_n[c]	$M_{n,NMR}$[d] (KDa)	N_{ATRP}[e]	D_{ATRP}[f] (%)
3a	0.7	12.34	5.7	1.18	10.4	16.2	52.3
3b	1.0	16.28	6.2	1.14	10.8	22.3	71.9

[a] Reaction temperature: 80 °C; reaction time: 24 h; feeding ratio: [methyl]:[BPO] = 1:0.2.
[b] Determined by the titration with $Hg(NO_3)_2$.
[c] Measured by GPC in THF at 35 °C.
[d] Determined by ^1H NMR.
[e] The number of ATRP initiation group per chain.
[f] Grafting density of ATRP initiation group.

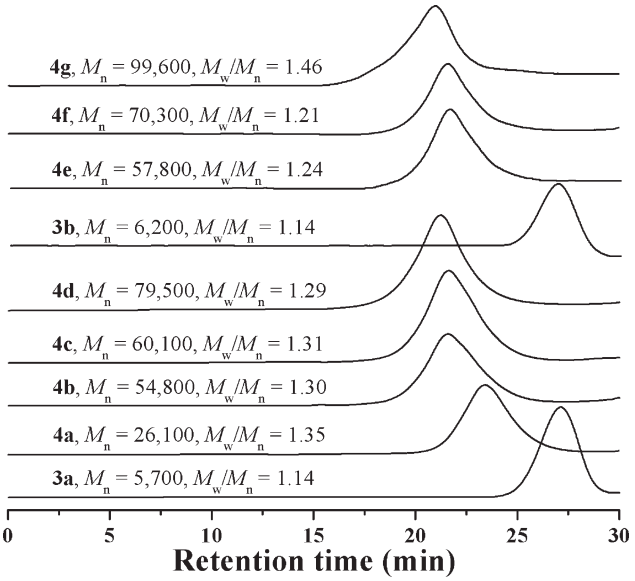

FIGURE 5 GPC traces of PMBTFVB-Br **3** and PMBTFVB-*g*-PMMA **4**.

calculated to be 52.3% = 16.2/31.0 and 71.9% = 22.3/31.0 for **3a** and **3b** macroinitiators (Table 1), respectively.

$$\begin{cases} \dfrac{80x}{363x + 284y + 204 \times 2} = Br\% & (2) \\ x + y = 31.0 & (3) \end{cases}$$

^{1}H NMR is used to determine the molecular weight of PMBTFVB-Br **3** macroinitiator ($M_{n,NMR}$) according to eq 4, in which S_a, S_b, and S_c are the area of peak "a" at 3.68 ppm, peaks "b" at 1.99 and 2.18 ppm, and peaks "c" at 4.17 and 4.34 ppm in Figure 3(B), respectively. The values are 10,400 g/mol for PMBTFVB-Br **3a** and 10,800 g/mol for PMBTFVB-Br **3b**, as listed in Table 1.

$$M_{n,NMR} = 363 \times (3S_c/S_a) + 284 \times (2S_b/S_a) + 204 \times 2 \quad (4)$$

Thus, it can be concluded from the above results that halogen-containing ATRP initiation sites have been successfully incorporated into the main chain without affecting the polymeric architecture, and 16.2 and 22.3 CH_2Br groups are involved in PMBTFVB-Br **3a** and **3b** macroinitiators, respectively.

Synthesis of PMBTFVB-*g*-PMMA Graft Copolymer

PMBTFVB-Br **3** macroinitiator initiated ATRP of MMA at 50 °C using CuBr/dHbpy as catalytic system to provide PMBTFVB-*g*-PMMA graft copolymers via the grafting-from strategy (Table 2). The molecular weights of graft copolymers were all much higher than those of macroinitiators, which demonstrated ATRP of MMA was performed and they also increased with the extending of polymerization time, which is the characteristic of ATRP.[53,54] In this case, a high feed ratio of MMA to the initiation group (250:1) and a relatively low conversion of MMA (<35%) were used to suppress the intermolecular coupling reactions according to previous reports.[43,66,79–84] All graft copolymers showed unimodal and symmetrical GPC curves (Fig. 5) with relatively narrow molecular weight distributions ($M_w/M_n \leq$ 1.46), which indicated that intermolecular coupling reactions could be neglected.[66]

FT-IR spectrum of PMBTFVB-*g*-PMMA **4** graft copolymer is shown in Figure 6. The sharp band of the carbonyl of PMMA side chains located at 1730 cm^{-1}. The peaks at 1483 and 1449 cm^{-1} were attributed to the benzene ring of PMBTFVB backbone. The characteristic signal of perfluorocyclobutyl unit appeared at 963 cm^{-1}. Figure 7(A) shows typical ^{1}H NMR signals of the corresponding protons of PMBTFVB backbone and PMMA side chains. The strong peak at 3.60 ppm originated from three protons of $COOCH_3$ group of PMMA side chain. The signal of three protons of CCH_3 group of PMMA side chains appeared at 0.84, 1.02, and 1.25 ppm. After graft copolymerization, the peaks of two protons of CH_2Br group connected to the benzene ring at 4.17 and 4.34 ppm in Figure 3(B) disappeared, which meant that every pendant ATRP initiation group initiated the polymerization of MMA and the signal of two protons of CH_2 connected to the benzene ring appeared at 1.89 ppm instead. The signal of three protons of terminal methoxyl of the backbone was still found to be located at 3.82 ppm. In addition, a series of

TABLE 2 Synthesis of PMBTFVB-*g*-PMMA **4** Graft Copolymer[a]

Sample	Time (h)	Conv.[d] (%)	$M_{n,GPC}$[e] (KDa)	M_w/M_n[e]	N_{MMA}[f]	n_{MMA}[g]	$M_{n,NMR}$[h] (KDa)
4a[b]	0.5	5.25	26.1	1.35	257.5	15.9	36.2
4b[b]	1.5	18.63	54.8	1.30	561.7	34.7	66.6
4c[b]	2.5	22.08	60.1	1.31	961.6	59.4	106.6
4d[b]	3.5	33.96	79.5	1.29	1673.1	103.3	177.7
4e[c]	1.5	11.55	57.8	1.24	543.6	24.4	65.2
4f[c]	2.5	23.68	70.3	1.21	839.3	37.6	94.7
4g[c]	3.5	34.13	99.6	1.46	1694.4	76.0	180.2

[a] Polymerization temperature: 50 °C; feeding ratio: [MMA]:[CH_2Br group]:[CuBr]:[dHbpy] = 250:1:1:2, V_{MMA}:$V_{anisole}$ = 1:1.
[b] Initiated by PMBTFVB-Br **3a**.
[c] Initiated by PMBTFVB-Br **3b**.
[d] Determined by GC using anisole as internal standard.
[e] Measured by GPC in THF at 35 °C.
[f] Total number of MMA repeating unit obtained from ^{1}H NMR.
[g] The number of MMA repeating unit per PMMA side chain obtained from ^{1}H NMR.
[h] Determined by ^{1}H NMR.

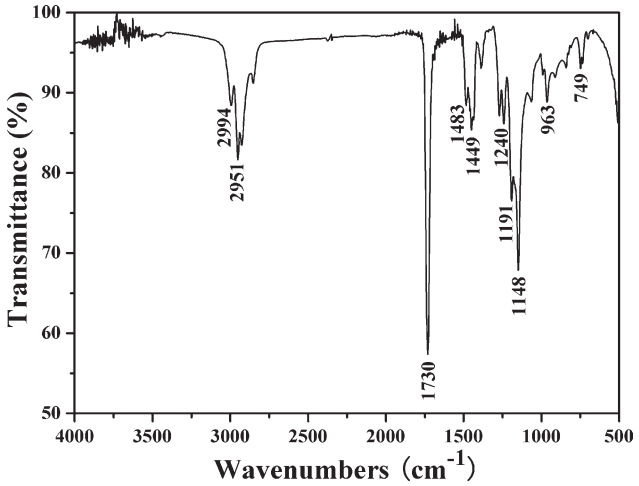

FIGURE 6 FT-IR spectrum of PMBTFVB-*g*-PMMA **4**.

peaks between −128.1 and −132.2 ppm appeared in ^{19}F NMR spectrum of PMBTFVB-*g*-PMMA **4** as shown in Figure 7(B), confirming the existence of PFCB linkage in the graft copolymer. All these points made sure of the structure of PMBTFVB-*g*-PMMA **4** graft copolymer.

Because the molecular weight of the graft copolymer measured by GPC is much lower than the "real" value,[85] ^1H NMR was used to determine the molecular weight of PMBTFVB-*g*-PMMA **4** graft copolymer ($M_{n,NMR}$) instead of GPC. The total number of MMA repeating unit (N_{MMA}), the molecular weight of the graft copolymer ($M_{n,NMR}$), and the number of MMA repeating unit per PMMA side chain (n_{MMA}) can be calculated according to eqs 5 (S_e and S_a are the area of peaks "e" at 0.84, 1.02, and 1.25 ppm and peak "a" at 3.82 ppm in Figure 7, respectively; 2 is the number of terminal methoxyl of the backbone), 6 ($M_{n,3}$ is the molecular weight of PMBTFVB-Br **3** macroinitiator as listed in Table 1 and 100 is the molecular weight of MMA), and 7 (N_{ATRP} is the number of grafted ATRP initiation group per chain as listed in Table 1), respectively. Indeed, the molecular weights determined by ^1H NMR (Table 2) are much higher than those obtained by GPC.

$$N_{MMA} = 2 \times (S_e/S_a) \quad (5)$$

$$M_{n,NMR} = M_{n,3} + 100 \times N_{MMA} \quad (6)$$

$$n_{MMA} = N_{MMA}/N_{ATRP} \quad (7)$$

The conversions of MMA were measured by GC (Table 2) and the semilogarithmic plots of $Ln([M]_0/[M])$ versus time were depicted in Figure 8. It is clear that $Ln([M]_0/[M])$ linearly depends on the time, indicating that the apparent polymerization rate is first order with respect to the concentration of MMA and the number of propagating species is constant during the polymerization. This phenomenon and seven unimodal and symmetrical GPC curves of PMBTFVB-*g*-

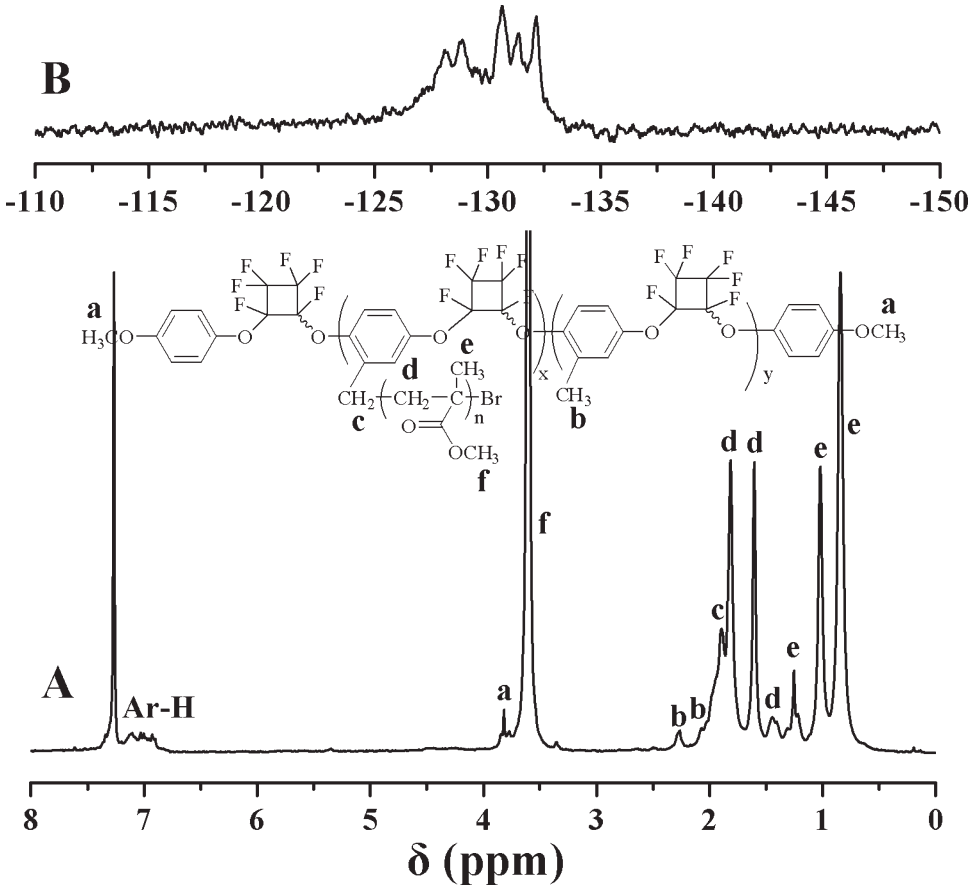

FIGURE 7 ^1H (A) and ^{19}F (B) NMR spectra of PMBTFVB-*g*-PMMA **4** in $CDCl_3$.

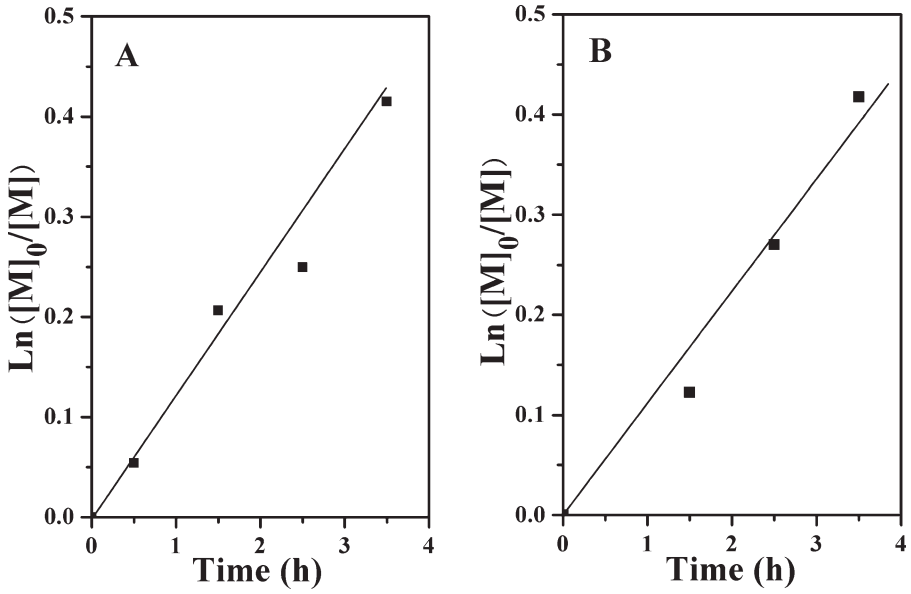

FIGURE 8 Kinetic plots for solution ATRP of MMA initiated by PMBTFVB **3a** and **3b** at 50 °C, [MMA]:[CH_2Br group]:[CuBr]:[dHbpy] = 250:1:1:2.

PMMA **4** graft copolymers with relatively narrow molecular weight distributions ($M_w/M_n \leq 1.46$) in Figure 5 both fit in with the characteristic of ATRP.[54,55] Thus, it can be concluded that a series of PMBTFVB-*g*-PMMA **4** graft copolymers consisting of a perfluorocyclobutyl aryl ether-based backbone possessing 31 repeating units and PMMA (15–103 repeating units per chain) side chains were successfully synthesized by the well-controlled ATRP of MMA initiated by PMBTFVB-Br **3** macroinitiator.

Properties of Graft Copolymer

PMBTFVB-*g*-PMMA **4** graft copolymers with different molecular weights exhibit excellent solubility in most common solvents including THF, CH_2Cl_2, chloroform, acetone, ethyl

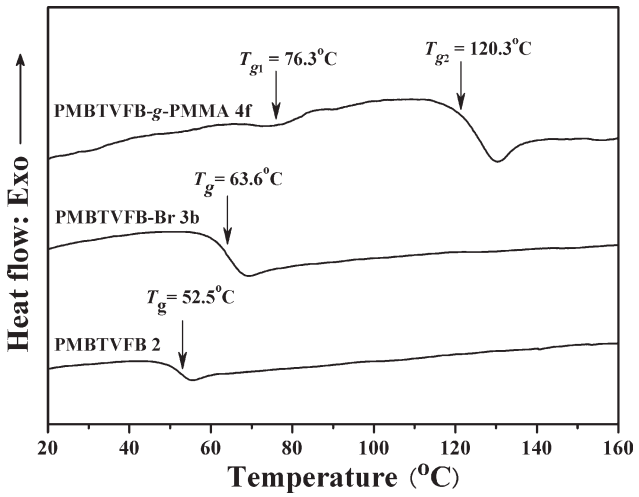

FIGURE 9 Third heating DSC scans (in N_2) of PMBTFVB **2**, PMBTFVB-Br **3b**, and PMBTFVB-*g*-PMMA **4f** with a heating rate of 10 °C/min.

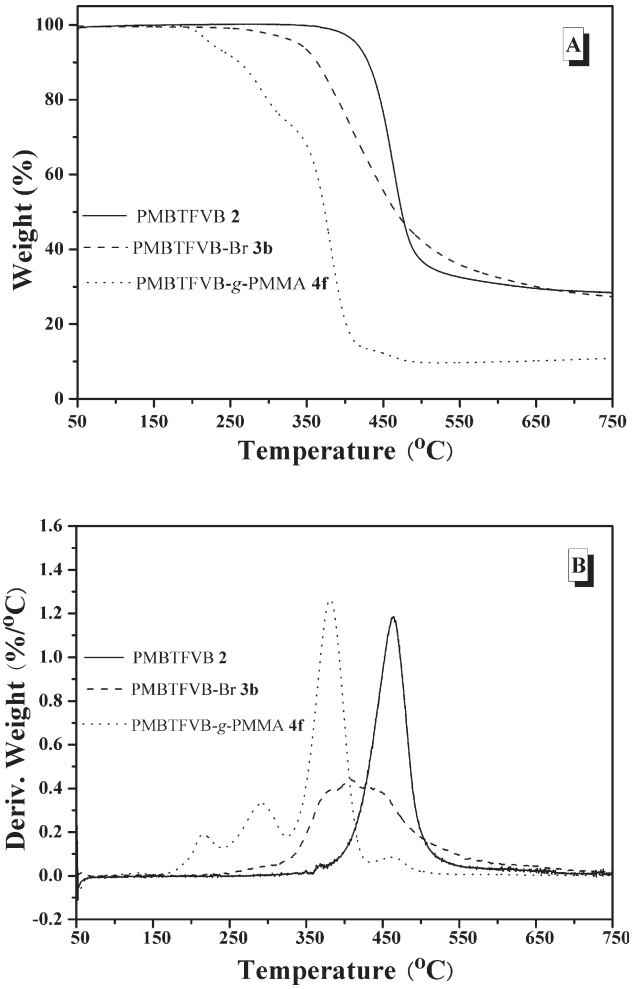

FIGURE 10 TG (A) and DTG (B) curves (in N_2) of PMBTFVB **2**, PMBTFVB-Br **3b**, and PMBTFVB-*g*-PMMA **4f** with a heating rate of 10 °C/min.

acetate, toluene, and DMF; however, it is insoluble in water and methanol.

DSC thermogram of PMBTFVB-*g*-PMMA **4f** graft copolymer is shown in Figure 9 and two T_gs were found to be located at 120.3 and 76.3 °C, respectively. The higher T_g at 120.3 °C obviously corresponded to PMMA side chains, which was similar to that of PMMA homopolymer.[86,87] The lower T_g at 76.3 °C was attributed to PMBTFVB backbone, which was much higher than those of PMBTFVB **2** homopolymer (T_g = 52.5 °C) and PMBTFVB-Br **3a** macroinitiator (T_g = 63.6 °C) as shown in Figure 9; this can be explained that the free rotation of PMBTFVB backbone was confined by PMMA branches. The presence of two different T_gs also indicated that a bulk microphase separation exist in PMBTFVB-*g*-PMMA **4** graft copolymer.[88,89]

Thermal stability of the polymers was measured by TGA and the typical TG (thermogravimetry) and DTG (derivative thermogravimetry) curves are shown in Figure 10. The pyrolysis of PMBTFVB **2** homopolymer and PMBTFVB-Br **3b** macroinitiator processed in a one-stage decomposition pattern and T_d of PMBTFVB **2** and PMBTFVB-Br **3b** are recorded at 431 and 364 °C respectively. However, the thermolysis of PMBTFVB-*g*-PMMA **4f** graft copolymer shows a multi-step degradation process around about 169 and 500 °C, which corresponded to the weight loss of PMMA branches[90,91] and PMBTFVB backbone, respectively.

CONCLUSIONS

In summary, we reported the first example of perfluorocyclobutyl aryl ether-based graft copolymer with relatively narrow molecular weight distributions ($M_w/M_n \leq 1.46$) synthesized by the sequential thermal step-growth cycloaddition polymerization of 2-methyl-1,4-bistrifluorovinyloxybenzene and ATRP of MMA. NBS and BPO were used to transform the pendant methyls on the perfluorocyclobutyl aryl ether-based backbone into ATRP initiation groups without affecting the main chain. The graft copolymers were obtained by the combination of the grafting-from strategy and ATRP of methyl methacrylate. The polymerization showed a first-order kinetics and the molecular weight of the graft copolymer increased with the raising of the polymerization time. These fluoropolymers show excellent solubility in common organic solvents.

The authors thank the financial support from National Natural Science Foundation of China (20674094, 21074145, 50873029, and 51073042), Shanghai Rising Star Program (07QA14066), and Shanghai Nano-Technology Program (0952nm05800).

REFERENCES AND NOTES

1 Babb, D. A.; Snelgrove, R. V.; Smith, D. W.; Mudrich, S. F. In Step-Growth Polymers for High-Performance Materials; American Chemical Society: Washington, DC, 1996; pp 431–441.

2 Plunkett, R. J. Polym Prepr 1986, 27, 485–487.

3 Percec, V.; Lee, M. J Macromol Sci Pure Appl Chem 1992, 29, 723–740.

4 Percec, V.; Schlueter, D.; Kwon, Y. K.; Blackwell, J.; Moller, M.; Slangen, P. J. Macromolecules 1995, 28, 8807–8818.

5 Johansson, G.; Percec, V.; Ungar, G.; Zhou, J. P. Macromolecules 1996, 29, 646–660.

6 Percec, V.; Johansson, G.; Ungar, G.; Zhou, J. P. J Am Chem Soc 1996, 118, 9855–9866.

7 Percec, V.; Schlueter, D.; Ungar, G. Macromolecules 1997, 30, 645–648.

8 Johansson, G.; Percec, V.; Ungar, G.; Smith, K. Chem Mater 1997, 9, 164–175.

9 Hudsom, S. D.; Jung, H. T.; Percec, V.; Cho, W. D.; Johanssom, G.; Ungar, G., Balagurusamy, V. S. K. Science 1997, 248, 449–452.

10 Percec, V.; Glodde, M.; Bera, T. K.; Miura, Y.; Shiyanovskaya, I.; Singer, K. D.; Balagurusamy, V. S. K.; Heiney, P. A.; Schnell, I.; Rapp, A.; Spiess, H. W.; Hudsonk, S. D.; Duank, H. Nature 2002, 419, 384–388.

11 Dukeson, D. R.; Ungar, G.; Balagurusamy, V. S. K.; Percec, V.; Johansson, G. A.; Glodde, M. J Am Chem Soc 2003, 125, 15974–15980.

12 Percec, V.; Imam, M. R.; Bera, T. K.; Balagurusamy, V. S. K.; Peterca, M.; Heiney, P. A. Angew Chem Int Ed 2005, 44, 4739–4745.

13 Percec, V.; Glodde, M.; Peterca, M.; Rapp, A.; Schnell, I.; Spiess, H. W.; Bera, T. K.; Miura, Y.; Balagurusamy, V. S. K.; Aqad, E.; Heiney, P. A. Chem Eur J 2006, 12, 6298–6314.

14 Percec, V.; Aqad, E.; Peterca, M.; Imam, M. R.; Glodde, M.; Bera, T. K.; Miura, Y.; Balagurusamy, V. S. K.; Ewbank, P. C.; Wurthner, F.; Heiney, P. A. Chem Eur J 2007, 13, 3330–3345.

15 Wilson, C. J.; Wilson, D. A.; Feiring, A. E.; Percec, V. J Polym Sci Part A: Polym Chem 2010, 48, 2498–2508.

16 Babb, D. A.; Ezzell, B. R.; Clement, K. S.; Richey, W. F.; Kennedy, A. P. J Polym Sci Part A: Polym Chem 1993, 31, 3465–3477.

17 Kennedy, A. P.; Babb, D. A.; Bermmer, J. N.; Pasztor, A. J. J Polym Sci Part A: Polym Chem 1995, 33, 1859–1865.

18 Smith, D. W.; Babb, D. A. Macromolecules 1996, 29, 852–860.

19 Smith, D. W.; Boone, H. W.; Traiphol, R.; Shah, H.; Perahia, D. Macromolecules 2000, 33, 1126–1128.

20 Jin, J. Y.; Topping, C. M.; Chen, S. R.; Ballato, J.; Foulger, S. H.; Smith, D. W. J Polym Sci Part A: Polym Chem 2004, 42, 5292–5300.

21 Feiring, A. E. In Organofluorine Chemistry: Principle and Commercial Applications; Banks, R. E.; Smart, B. E.; Tatlow, J. C., Eds.; Plenum Press: New York, 1994; pp 339–371.

22 Yamabe, M. In Organofluorine Chemistry: Principle and Commercial Applications; Banks, R. E.; Smart, B. E.; Tatlow, J. C., Eds.; Plenum Press: New York, 1994; pp 397–402.

23 Resnick, P. R.; Buck, W. H. In Modern Fluoropolymers: High Performance Polymers for Diverse Applications; Schirs, J., Ed.; Wiley: New York, 1997; pp 397–420.

24 Iacono, S. T.; Budy, S. M.; Jin, J. Y.; Smith, D. W. J Polym Sci Part A: Polym Chem 2007, 45, 5705–5721.

25 Liu, S.; Jiang, X. Z.; Ma, H.; Liu, M. S.; Jen, A. K. Y. Macromolecules 2000, 33, 3514–3517.

26 Jiang, X. Z.; Liu, S.; Liu, M. S.; Herguth, P.; Jen, A. K. Y.; Sarikaya, M. Adv Funct Mater 2002, 12, 745–751.

27 Smith, D. W.; Chen, S. R.; Kumar, S. M.; Ballato, J.; Topping, C.; Shah, H. V.; Foulger, S. H. Adv Mater 2002, 14, 1585–1589.

28 Wong, S.; Ma, H.; Jen, A. K. Y.; Barto, R.; Frank, C. W. Macromolecules 2003, 36, 8001–8007.

29 Lin, Y. B.; Rahmanian, N.; Kim, S. H.; Nordin, G. P.; Topping, C.; Smith, D. W.; Ballato, J. J Lightwave Technol 2008, 26, 3062–3070.

30 Ghim, J.; Shim, H. S.; Shin, B. G.; Park, J. H.; Hwang, J. T.; Chun, C.; Oh, S. H.; Kim, J. J.; Kim, D. Y. Macromolecules 2005, 38, 8278–8284.

31 Jin, J. Y.; Smith, D. W.; Glasser, S.; Perahia, D.; Foulger, S. H.; Ballato, J.; Kang, S. W.; Kumar, S. Macromolecules 2006, 39, 4646–4649.

32 Iacono, S. T.; Budy, S. M.; Ewald, D.; Smith, D. W. Chem Commun 2006, 4844–4846.

33 Cho, S. Y.; Allcock, H. R. Chem Mater 2007, 19, 6338–6344.

34 Campbell, V. E.; Paoprasert, P.; Mykietyn, J. D.; In, I.; McGee, D. J.; Gopalan, P. J Polym Sci Part A: Polym Chem 2007, 45, 3166–3177.

35 Iacono, S. T.; Budy, S. M.; Mabry, J. M.; Smith, D. W. Macromolecules 2007, 40, 9517–9522.

36 Qian, G. Q.; Smith, D. W.; Benicewicz, B. C. Polymer 2009, 50, 3911–3916.

37 Neilson, A. R.; Budy, S. M.; Ballato, J. M.; Smith, D. W. Macromolecules 2007, 40, 9378–9383.

38 Budy, S. M.; Suresh, S.; Spraul, B. K.; Smith, D. W. J Phys Chem C 2008, 112, 8099–8104.

39 Huang, X. Y.; Lu, G. L.; Peng, D.; Zhang, S.; Qing, F. L. Macromolecules 2005, 38, 7299–7305.

40 Lu, G. L.; Zhang, S.; Huang, X. Y. J Polym Sci Part A: Polym Chem 2006, 44, 5438–5444.

41 Zhu, Y. Q.; Huang, Y. G.; Meng, W. D.; Li, H. Q.; Qing, F. L. Polymer 2006, 47, 6272–6279.

42 Yao, R. X.; Kong, L.; Yin, Z. S.; Qing, F. L. J Fluorine Chem 2008, 129, 1003–1010.

43 Zhang, M. F.; Breiner, T.; Mori, H.; Muller, A. H. E. Polymer 2003, 44, 1449–1458.

44 Dziezok, P.; Sheiko, S. S.; Fischer, K.; Schmidt, M.; Moller, M. Angew Chem Int Ed 1997, 36, 2812–2815.

45 Heroguez, V.; Gnanou, Y.; Fontanille, M. Macromolecules 1997, 30, 4791–4798.

46 Deffieux, A.; Schappacher, M. Macromolecules 1999, 32, 1797–1802.

47 Gao, H. F.; Matyjaszewski, K. J Am Chem Soc 2007, 129, 6633–6639.

48 Fu, Q.; Lin, W. C.; Huang, J. L. Macromolecules 2008, 41, 2381–2387.

49 Engler, A. C.; Lee, H. I.; Hammond, P. T. Angew Chem Int Ed 2009, 48, 9334–9338.

50 Durmaz, Y. Y.; Kumbaraci, V.; Demirel, A. L.; Talinli, N.; Yagci, Y. Macromolecules 2009, 42, 3743–3749.

51 Li, Y. G.; Zhang, Y. Q.; Yang, D.; Li, Y. J.; Hu, J. H.; Feng, C.; Zhai, S. J.; Lu, G. L.; Huang, X. Y. Macromolecules 2010, 43, 262–270.

52 Beers, K. L.; Gaynor, S. G.; Matyjaszewski, K.; Sheiko, S. S.; Moller, M. Macromolecules 1998, 31, 9413–9415.

53 Matyjaszewski, K.; Xia, J. H. Chem Rev 2001, 101, 2921–2990.

54 Wang, J. S.; Matyjaszewski, K. J Am Chem Soc 1995, 117, 5614–5615.

55 Wang, J. S.; Matyjaszewski, K. Macromolecules 1995, 28, 7901–7910.

56 Percec, V.; Barboiu, B. Macromolecules 1995, 28, 7970–7972.

57 Kato, M.; Kamigaito, M.; Sawamoto, M.; Higashimura, T. Macromolecules 1995, 28, 1721–1723.

58 Jakubowski, W.; Matyjaszewski, K. Angew Chem Int Ed 2006, 45, 4482–4486.

59 Percec, V.; Guliashvili, T.; Ladislaw, J. S.; Wistrand, A.; Stjerndahl, A.; Sienkowska, M. J.; Monteiro, M. J.; Sahoo, S. J Am Chem Soc 2006, 128, 14156–14165.

60 Nguyen, N. H.; Rosen, B. M.; Lligadas, G.; Percec, V. Macromolecules 2009, 42, 2379–2386.

61 Rosen, B. M.; Percec, V. Chem Rev 2009, 109, 5069–5119.

62 Fleischmann, S.; Rosen, B. M.; Percec, V. J Polym Sci Part A: Polym Chem 2010, 48, 1990–1996.

63 Fleischmann, S.; Percec, V. J Polym Sci Part A: Polym Chem 2010, 48, 2236–2242.

64 Moad, G.; Rizzardo, E.; Thang, S. H. Polymer 2008, 49, 1079–1131.

65 Moad, G.; Rizzardo, E.; Thang, S. H. Acc Chem Res 2008, 41, 1133–1142.

66 Cheng, G. L.; Boker, A.; Zhang, M. F.; Krausch, G.; Muller, A. H. E. Macromolecules 2001, 34, 6883–6888.

67 Cheng, C.; Khoshde, E.; Wooley, K. L. Nano Lett 2006, 6, 1741–1746.

68 Hans, M.; Keul, H.; Heise, A.; Moeller, M. Macromolecules 2007, 40, 8872–8880.

69 Yuan, W. Z.; Yuan, J. Y.; Zhang, F. B.; Xie, X. M.; Pan, C. Y. Macromolecules 2007, 40, 9094–9102.

70 Touris, A.; Kostakis, K.; Mourmouris, S.; Kotzabasakis, V.; Pitsikalis, M.; Hadjichristidis, N. Macromolecules 2008, 41, 2426–2438.

71 Wang, M. F.; Zou, S.; Guerin, G.; Shen, L.; Deng, K. Q.; Jones, M.; Walker, G. C.; Scholes, G. D.; Winnik, M. A. Macromolecules 2008, 41, 6993–7002.

72 Allen, M. J.; Wangkanont, K.; Raines, R. T.; Kiessling, L. L. Macromolecules 2009, 42, 4023–4027.

73 Zhang, Y. Q.; Shen, Z.; Yang, D.; Feng, C.; Hu, J. H.; Lu, G. L.; Huang, X. Y. Macromolecules 2010, 43, 117–125.

74 Kastsuhara, Y.; DesMarteau, D. D. J Am Chem Soc 1980, 102, 2681–2686.

75 Leduc, M. R.; Hawker, C. I.; Dao, J.; Frechet, J. M. J. J Am Chem Soc 1996, 118, 11111–11118.

76 Jin, J. Y.; Topping, C. M.; Suresh, S.; Foulger, S. H.; Rice, N.; Mojazza, B. H.; Smith, D. W. Polymer 2005, 46, 6923–6932.

77 Iacono, S. T.; Budy, S. M.; Mabry, J. M.; Smith, D. W. Polymer 2007, 48, 4637–4645.

78 Neilson, A. R.; Budy, S. M.; Ballato, J. M.; Smith, D. W. Polymer 2008, 49, 3228–3232.

79 Peng, D.; Zhang, X. H.; Huang, X. Y. Macromolecules 2006, 39, 4945–4947.

80 Gu, L. N.; Shen, Z.; Zhang, S.; Lu, G. L.; Zhang, X. H.; Huang, X. Y. Macromolecules 2007, 40, 4486–4493.

81 Liu, S. S.; Ayusman, S. Macromolecules 2000, 33, 5106–5110.

82 Borner, H. G.; Beers, K.; Matyjaszewski, K. Macromolecules 2001, 34, 4375–4383.

83 Matyjaszewski, K.; Qin, S. H.; Boyce, J. R.; Shirvanyants, D.; Sheiko, S. S. Macromolecules 2003, 36, 1843–1849.

84 Shen, Z.; Chen, Y.; Barriau, E.; Frey, H. Macromol Chem Phys 2006, 207, 57–64.

85 Jia, Z. F.; Fu, Q.; Huang, J. L. Macromolecules 2006, 39, 5190–5193.

86 Wu, S. H. J Appl Polym Sci 1992, 46, 619–624.

87 Pomposo, J. A.; Eguiazabal, I.; Calahorra, E.; Cortazar, M. Polymer 1993, 34, 95–102.

88 Zhang, X. H.; Shen, Z.; Li, L. T.; Zhang, S.; Lu, G. L.; Huang, X. Y. J Polym Sci Part A: Polym Chem 2007, 45, 5509–5517.

89 Zhang, X. H.; Shen, Z.; Li, L. T.; Lu, G. L.; Gu, L. N.; Huang, X. Y. Polymer 2007, 48, 5507–5513.

90 Singha, N. K.; German, A. L. J Appl Polym Sci 2007, 103, 3857–3864.

91 Granel, C.; Dubois, P.; Jerome, R.; Teyssie, P. Marcomolecules 1996, 29, 8576–8582.